Cellulose (2013) 20:303–313
DOI 10.1007/s10570-012-9815-0

ORIGINAL PAPER

Resin impregnation of cellulose nanofibril films facilitated by water swelling

Yan Qing · Ronald Sabo · Zhiyong Cai · Yiqiang Wu

Received: 17 August 2012/Accepted: 24 October 2012/Published online: 8 November 2012

Abstract Flexible composite films were produced by impregnating aqueous phenol formaldehyde (PF) resin into water-swollen cellulose nanofibril (CNF) films. CNF films were prepared using a pressurized filtration method in combination with freeze drying. The freeze-dried films were swollen with water then impregnated with PF resin by soaking in aqueous resin solutions of varying concentrations. Small amounts of PF slightly enhanced the tensile properties of CNF films. The formulation with the best mechanical properties was CNF/PF films with 8 wt % resin exhibiting tensile stress and toughness of 248 MPa and 26 MJ/m^3, respectively. Resin concentrations higher than about 8 % resulted in composites with decreased tensile properties as compared to neat CNF films. The wet strength of the composite films was significantly higher than that of the neat CNF films. The resulting composites showed greater resistance to moisture absorption accompanied by reduced thickness swelling when soaked in water as compared to neat CNF films. The composites also showed decreased oxygen permeability at low humidity compared to neat films, but the composites did not show improved barrier properties at high humidity.

Keywords Cellulose nanofibril · Phenol formaldehyde · Water swelling · Mechanical properties · Wet strength · Morphology · Oxygen permeability

Y. Qing · Y. Wu (*)
School of Materials Science and Engineering, Central South University of Forestry and Technology, 498 Shaoshan South Road, Changsha 410004, China
e-mail: wuyiqiang@csuft.edu.cn

Y. Qing · R. Sabo · Z. Cai (*)
Forest Products Laboratory, United States Department of Agriculture, 1 Gifford Pinchot Drive, Madison 53726-2398, WI, USA
e-mail: zcai@fs.fed.us

Introduction

Cellulose nanofibril (CNF) has recently been receiving increased attention for their use in composite materials (Sir6 and Plackett 2010). These nano-scale fibers have been reported to have remarkable mechanical properties, including an elastic modulus measured to be about 150 GPa (Iwamoto et al. 2009). Such mechanical properties suggest that CNF has the potential to compete with other inorganic reinforcements, such as glass fibers. In addition, films and composites made from CNFs have low thermal expansion (Nogi et al. 2009), provide effective gas and oil barrier (Syverud and Stenius 2009 ; Aulin et al. 2010; Rodionova et al. 2012), and exhibit excellent light transparency (Nogi et al. 2009 ; Zhu et al. 2011). The particular mechanical and physical properties of cellulose nanofibrils lend themselves to a wide range of potential applications, including packaging and coatings (Syverud and Stenius

2009; Aulin et al. 2010), reinforced nanocomposites (Svagan et al. 2007; Iwatake et al. 2008; Gong et al. 2011), conductive substrates (Nyström et al. 2010 Sasso et al. 2010), stiff magnetic nanopapers (Olsson et al. 2010) multi-functional aerogels (Pääkkö et al. 2008), and biomedical applications (Czaja et al. 2007).

Strong, flexible, water-resistant barrier composite films are of interest for applications including packaging and electronics. Numerous studies have shown that CNF films have good barrier properties at low humidity (Minelli et al. 2010; Syverud and Stenius 2009; Fukuzumi et al. 2009; Aulin et al. 2010), but these barrier properties tend to deteriorate at high humidity (Minelli et al. 2010; Syverud and Stenius 2009; Aulin et al. 2010). There are essentially two approaches that have been employed to reduce the moisture absorption of cellulose nanofibrils films. One approach involves modifications which convert the hydrophilic groups on nanofibrils into hydrophobic ones using functional treatments, such as surface silylation (Andresen et al. 2006; Lu et al. 2008) and acetylation (Tingaut et al. 2010). The chemical treatments significantly decrease surface energy and wettability, and lead to improved water-resistance. Another approach is the incorporation of resins with CNFs, which has been shown to reduce the amount of moisture absorption in the resulting composite (Heriksson et al. 2008; Qing et al. 2012), thus providing the potential to improve the barrier properties of CNF composites at high humidity.

Various cellulose nanofibril films and laminate composites, reinforced with different resins have previously been reported. For example, CNF-acrylic resin composites were successfully prepared as alternative materials for organic light-emitting diode displays (Okahisa et al. 2009). Nakagaito and Yano (2005) reported that layered CNFPF composites had mechanical properties similar to magnesium alloy with a bending strength and Young's modulus of 370 MPa and 16 GPa, respectively. In another study, extremely low coefficients of thermal expansion (CTE) were obtained from CNF composites with 40 wt % PF (Nakagaito and Yano 2008). Furthermore, transparent CNF/epoxy composite films with excellent thermal conductivity and low thermal expansion were produced, and which showed promise for applications such as integrated circuits (Shimazaki et al. 2007) or flexible electronics (Sabo et al. 2012).

Despite the potential for CNF films and the reinforced composites, some of the procedures involve using solvents, along with vacuum impregnation or other cumbersome techniques. Furthermore, the water resistance of these composites has not been thoroughly studied despite the extremely hygroscopic nature of cellulose nanofibrils. We previously reported a simple method for making CNF/PF composites by mixing water-soluble PF resin and CNF suspensions prior to membrane filtration (Qing et al. 2012), and here we offer another simple alternative for impregnating CNF films with PF resin by first swelling the films with water. The physical, mechanical and morphological properties of the resulting composite films are reported. Additionally, the wet strength, moisture and water sorption, and oxygen permeation at low and high humidity for the composite films are evaluated.

Materials and methods

Materials

TEMPO oxidized cellulose nanofibrils used in this experiment were prepared according to the work reported by Saito et al. (2009), as briefly described here. Commercially-supplied fully bleached eucalyptus pulp was carboxylated using 2,2,6,6-tetramethylpiperidinyl-1-oxyl (TEMPO), sodium chlorite and sodium hypochlorite as the reactants at 60 °C for 48 h. TEMPO-oxidized pulp fibers were then washed thoroughly using deionized water and homogenized in a disperser to break apart fiber bundles. The fiber slurry was diluted to facilitate separation of coarse and fine fractions by centrifuging at 12 000 g, and the coarse fraction was rejected. The nanofibril suspension was concentrated to a solid content of approximately 0.4 % using an osmotic filtration system. A final clarification step was performed in which the nanofibril dispersion was passed once through an M-110EH-30 Microfluidizer (Microfluidics, Newton, MA, USA) with 200- and 87-µm chambers in series. The obtained carboxylated nanofibril suspension was stored at 4 °C without any drying until future utilization.

The water-soluble PF resin was a commercially available adhesive for fiberboard manufacture, which was provided by Georgia-Pacific Chemicals LLC and had a solid content of 50.5 %. When preparing the various PF resin solutions used in this study, the original adhesive was diluted with deionized water and vigorously stirred for 10 min.

Preparation of CNF and CNFPF composite films

The stock CNF suspensions were diluted with deionized water to about 0.2 wt % and stirred for about 2 h before filtration. The suspensions were filtered at room temperature under air pressure of 0.6 MPa for 10 h in a Hazardous Waste Filtration (YT30 142HW, Millipore Corporation, USA) with a stainless steel cylinder of 142 mm in diameter. The filtration Membrane (JVWP14225, Millipore Corporation, USA) had a reported pore size of 0.1 μm and was supported by filter paper (P2, Fisher Scientific, USA). The wet films were easily separated from the membranes and had a solid content of about 14 %. These films were then freeze-dried under vacuum pressure of 0.01 MPa with a cooling coil temperature of −60°C for 10 h using a Labconco (Kansas City, MO, USA) freeze-drying system.

To produce CNFPF composites, the freeze-dried films were initially soaked in deionized water for 2 h to facilitate swelling, and were then soaked in a 5, 10, 15 or 20 % PF resin solution for 22 h. A control CNF film was also soaked in deionized water. All the impregnations were performed at room temperature without any heating, vacuum or air pressure. After impregnation, films were washed carefully with deionized water to remove excess PF deposited on the surface. The rinsed films were air-dried for 2 h then placed between wax-coated papers and filter papers to remove excess water. When the solids content of the films reached about 30 %, the wax and filter papers were replaced with dry ones. The assembly was then sandwiched between two steel plates, and a 23 kg weight was placed on the plates to minimize deformation. When the CNF films reached about 80–90% solids content, they were then put into an oven at 50 °C for 8 h and conditioned in a humidity chamber at 50 % relative humidity (RH) and 27 °C for at least 24 h. Finally, the conditioned films were hot pressed at 130 °C for 2 min at 30 MPa of pressure between two special steel plates with reported surface roughness of 0.2 nm.

Characterization of CNF and CNF/PF composite films

Dry and wet tensile tests

Dry tensile properties of CNF films and CNFPF composites were tested according to ASTM D638-10 (2010a), and performed in an Instron 5865 universal materials testing machine with a 500 N load cell. The specimens were cut to conform to ASTM D638-10 type V dogbone shape using a die (Qualitest, Ft. Lauderdale, FL, USA), and the thickness ranging from 0.10 to 0.13 mm. All samples were conditioned at 50 % RH and 27 °C for 1 week before testing. The tests were conducted at cross-head speed of 1 mm/min in a room conditioned at 50 % RH and 23 °C, and the specimens were pre-loaded at 10 N to remove slack. At least 5 specimens were tested for each condition. Extension was taken to be the cross-head displacement, and the gage length was taken to be the narrow section of the dog-bone specimens. The toughness was calculated by numerical integration of the stress–strain curve. Modulus of elasticity was calculated as the slope of the stress–strain curve in the stress region of 30–70MPa. Film density was calculated gravimetrically by measuring the dimension and weight of multiple well-defined section of each film.

The wet tensile strength was tested in a method similar to the dry one. Dogbone shaped specimens were first soaked in deionized water at room temperature for 2.5, 5, 10 and 20 min respectively. After removing excess water on the surface, the soaked samples were placed between blot papers, and then immediately attached to the test fixture clips. Because there was significant difference between thicknesses after water swelling, the maximum load and elongation at break were estimated to characterize the wet strength. Extensions were taken to be the cross-head displacements and the gage length was 25.4 mm.

Morphological observation

Cross-section and fracture surfaces for CNF and CNF/PF films were examined using a Zeiss EVO40 scanning electron microscope (Carl Zeiss SMT, INC., Thornwood, NY, USA). The cross surface of films were cut by using an ultramicrotome fitted with a diamond knife, and fracture surfaces were obtained by tearing notched samples. The specimens were fixed onto a carbon tape substrate and coated with in a thin layer of gold–palladium alloy.

The Atomic Force Microscopy (AFM) scans were performed on the surface of the films using a Quesant (Agoura Hills, CA, USA) atomic force microscope in tapping mode. The scan size was 40 μm × 40 μm at a scan rate of 4 Hz and a resolution of 600 lines × 600

points. Small rectangular samples (approximately 3 mm x 3 mm) were affixed to AFM stubs using a two-part epoxy. Four locations on each specimen were scanned and averaged for surface roughness calculations.

Hygroscopic properties

Moisture absorption and water swelling behavior were used to characterize the hygroscopic performance of CNF and CNF/PF films. For moisture absorption, rectangular specimens (20 mm length x 6 mm width x 0.10–0.13 mm thickness) were equilibrated sequentially at 30, 65 and 90 % RH, and then again to 65 and 30 % RH, followed by oven drying at a temperature of 105 °C for 4 h. The samples were maintained at 27 °C and conditioned at each humidity level for at least 5 days until reaching equilibrium. A minimum of 5 specimens were tested, and the average value was used. For water absorption, rectangular specimens (20 mm length x 6 mm width x 0.10–0.13 mm thickness) were soaked in deionized water at room temperature, and water absorption was measured gravimetrically in an interval of half an hour until kept stable.

Oxygen permeability testing

Oxygen permeability testing was performed on neat films and on composite films soaked in 10 % PF resin (CNF10) according to ASTM D3985-05el (2010b) by MOCON Testing Services (Minneapolis, MN, USA) at 35 and 100 % RH. The testing at 35 % RH was done on a MOCON Oxtran 2/21 L Module Oxygen Permeability Instrument, and the testing at 100 % RH was done on a MOCON Oxtran 210 Oxygen Permeability Instrument. All tests were done in duplicate. The thickness of the tested films was 61 ± 1 μm.

Results and discussion

Attempts to directly impregnate freeze-dried CNF films with PF resin by soaking them in dilute aqueous solutions (from 5 to 20 % PF resin) resulted in insufficient levels of resin being impregnated. Wet CNF hydrogel films taken from the filtration apparatus were directly freeze-dried to produce porous films with the expectation that this porosity would facilitate resin impregnation. However, even after several days of soaking, no significant impregnation of resin into the films was observed. Furthermore, the presence of PF resin at concentrations as low as 5 % inhibited the absorption of water into the CNF films compared to films soaked in deionized water. Direct impregnation of dried films by soaking in aqueous PF resin solutions was difficult, which is why others have used a combination of solvents and vacuum pressure to facilitate the impregnation (Nakagaito and Yano 2005, 2008; Henriksson and Berglund 2007).

Here, we present a method in which water-soluble PF resin is readily impregnated into the CNF sheets by first swelling them in water followed by soaking them in PF resin solutions. Various properties of the composite films, including tensile properties, wet strength, distribution of PF, morphology, hygroscopic characteristic, and oxygen permeability are reported.

Swelling and impregnation CNF films

Freeze-dried CNF films with porosity of 8-10 % were immersed into PF resin with contents ranging from 5 to 20 %. Figure 1a shows CNF films soaked in deionized water, 5 % PF resin and 10 % PF resin for 2 h. Significant differences in thickness between the sample soaked in deionized water and those soaked in resin solutions are obvious. The CNF films soaked in water swelled approximately 10-fold from their original dry state. On the contrary, films soaked in PF solution swelled to only 2-3 times the original films. The weight increase of CNF films soaked in water (25 times the original films) was 3-4 times higher than those soaked in PF resin solutions (6-7 times the original films), although there were only slight differences between CNF films soaked in 5 and 10 % PF solutions. Figure 1b, c show CNF films that were soaked in 5 and 10 % PF resin for 24 h. The dark samples were first swollen in water for 2 h, and bright ones were only soaked in PF resin. Clearly, the samples soaked in resin without first being swollen with water did not absorb as much resin. Interestingly, the thicknesses of water-swollen films deceased gradually with resin impregnation time and exhibited the same thickness as the ones soaked in PF resin solution without previous water swelling (Fig. 1b, c). This is attributed to the migration of water attempting to reduce the osmotic pressure differential caused by the PF concentration gradient between the inner and

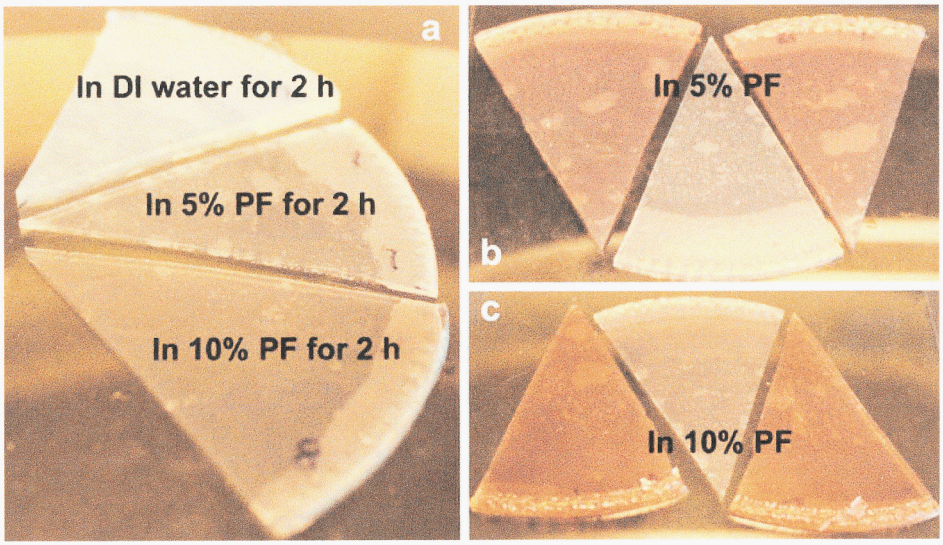

Fig. 1 Photographs of CNF films soaked in deionized (DI) water or PF resin solutions. a samples were soaked in water or resin solutions for 2 h, (b) and (c) samples were soaked in 5 and 10 % PF resin respectively. In (b) and (c), the dark films were first swelled in DI water for 2 h then soaked in the resin solutions for 22 h; the light-colored films in the middle were soaked in a resin solution for 24 h

outer layers of the films (Procter 1914). The final PF contents were 3–5% for original CNF films and up to 31 % for water swelled CNF films.

The swelling behavior of CNF films is complicated, and currently it is not exactly clear how swelling occurs at the molecular level (Aulin et al. 2009). However, a highlighted finding reported by Pizzi and Eaton (1987) provides a possible interpretation for the difference of CNF swelling in deionized water compared to swelling in PF resin solution. In cellulose, even for crystalline cellulose in a solvated state, the PF molecules were likely to displace water to adhere to the cellulose surface. Therefore, the strong adhesion of PF molecules to cellulose nanofibrils reduced exposure to water, and restricted further hydrogen bonds from being broken between adjacent nanofibrils. As a result, extra water and PF molecules were unable to permeate through CNF films. For the water-swollen CNF films, hydrogen bonds between nanofibrils were already replaced by bonds between water-nanofibrils (Aulin et al. 2010), and inner spacing and voids were expanded after swelling. This expansion allowed PF molecules to freely penetrate into CNF sheets.

The ultimate PF contents in CNF/PF composite films are shown in Table 1. For ease of discussion, the obtained CNF films soaked in deionized water and water-swelled CNF sheets soaked in 5, 10, 15 and 20 % PF resin are labeled as CNF, CNF5, CNF10, CNF15 and CNF20, respectively. Final resin concentrations in the hot-pressed composite films correlated with the concentration of resin in the soaking solution, and the resulting composite with the highest resin contained 31 % PF after soaking in a 20 % PF resin solution. This indicated that more PF molecules transferred into swelled CNF films under concentration differential. When drying in ambient conditions, films soaked in high concentration of PF resin (15 and 20 %) even had excessive PF leach out of them. The final PF contents in the composites were not predictable a priori based on resin concentration, film properties or impregnation conditions, but the concentration clearly correlates with impregnation solution concentration.

Morphological characterization

The SEM images of cross and fracture surfaces for CNF and CNF5 composite films are shown in Fig. 2. PF resin appears well distributed between nanofiber layers. The layered structure of CNF films is clearly visible, and the swelling of the films with water results in significant thickness increase but essentially negligible lateral swell. Therefore, the swelling seems to facilitate diffusion and deposition of PF resin monomers between the layers of CNFs. Figure 3 also shows fairly uniform resin coverage on the surface of the

Table 1 Physical and mechanical properties for CNF and CNF/PF composite films

Sample conditions	Sample ID	PF content (%)	Density (kg/m^3)	Strain at break (%)	Stress at yield (MPa)	Stress at break (MPa)	Tensile Young's modulus (GPa)	Toughness (m/m^3)
In water	CNF	0	1456 ± 18	14.4 ± 2.8	135 ± 7	216 ± 18	4.63 ± 0.15	23.0 ± 6.0
In 5 % PF	CNF5	8	1484 ± 19	14.7 ± 5.9	151 ± 8	248 ± 15	4.93 ± 0.14	26.4 ± 5.3
In 10 %PF	CNF10	15	1474 ± 21	10.1 ± 2.2	172 ± 5	227 ± 13	4.88 ± 0.10	16.9 ± 4.7
In 15 %PF	CNF15	28	1425 ± 10	4.9 ± 0.9	184 ± 17	184 ± 17	4.46 ± 0.07	5.8 ± 1.6
In 20 % PF	CNF20	31	1427 ± 6	4.5 ± 1.3	180 ± 25	180 ± 25	4.52 ± 0.11	5.3 ± 2.3

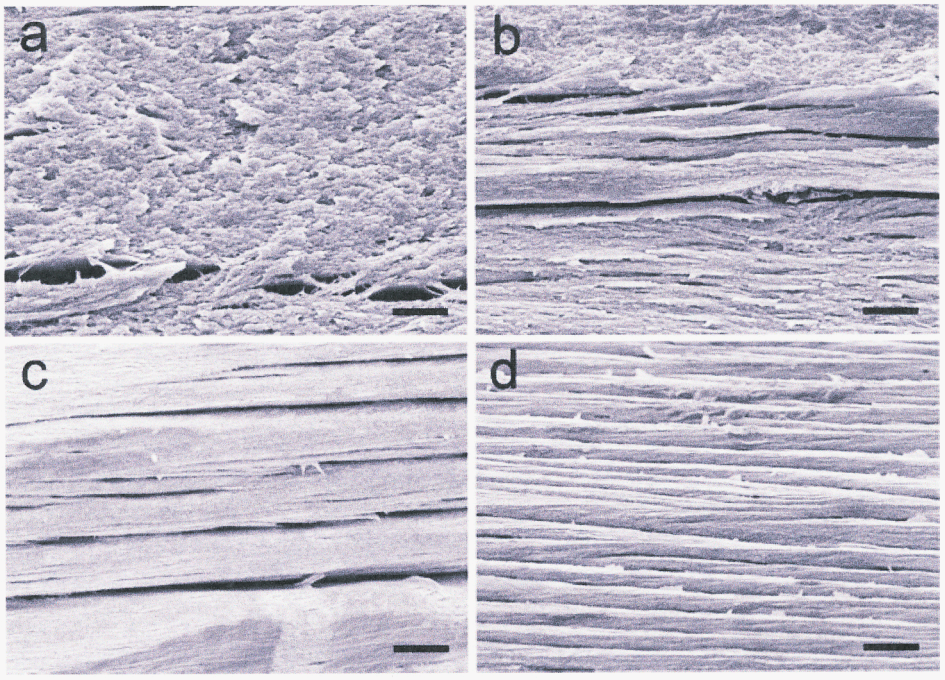

Fig. 2 SEM images of the cross surface (a and b) and fracture surface (**c** and **d**) for CNF (**a** and **c**) and CNF5 composite (**b** and **d**) films The scale bar for these images is 5 μm

composite films. These micrographs suggest that resin penetrates the film between layers and is well-dispersed, and this is further supported by the enhanced resilience of the composites, as previously mentioned.

Dry and wet tensile properties

Typical dry tensile curves for CNF and CNF/PF composite films are shown in Fig. 4, and detailed tensile properties are given in Table 1. Significant differences were observed between CNF films and CNF/PF composite films with high resin concentrations. Particularly, the stress and strain at break was considerably less for the composites with more than 15 wt % PF resin, making these composites with high resin content more brittle than neat films and those with low resin content. However, the yield stress for the neat films was considerably less than for the composites (seen in Table 1). The impregnation of PF resin into the CNF appears to make the composite films more resilient than the neat films. This likely indicates that good adhesion is obtained between the resin and the CNF fibers.

Interestingly, neat CNF films and CNF/PF films with low resin content (15 % or less) had high toughness, ranging from 17 to 26 MJ/m^3. Henriksson and Berglund (2007) reported cellulose nanopapers

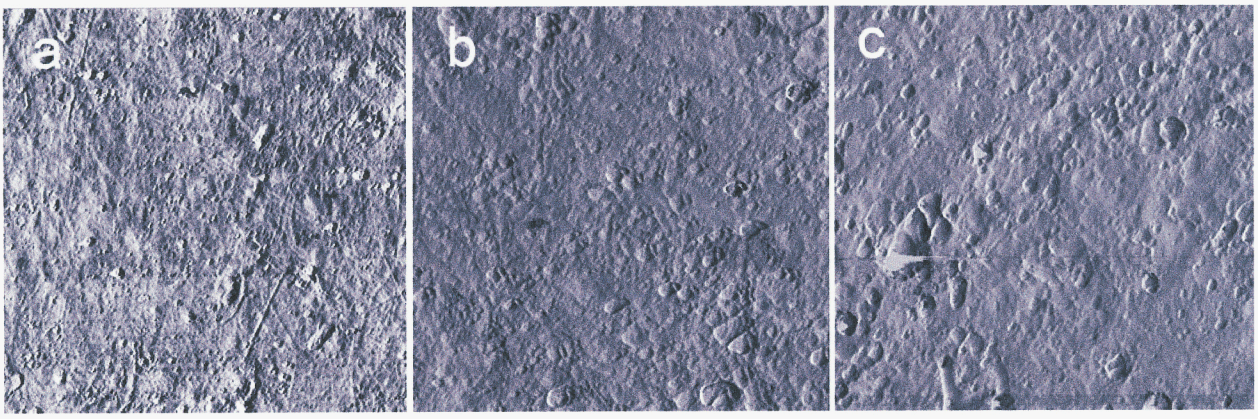

Fig. 3 AFM phase images of the surface of neat CNF (**a**) and CNF5 (**b**) and CNF10 (**c**). The scan area for these images is 40 µm x 40 µm

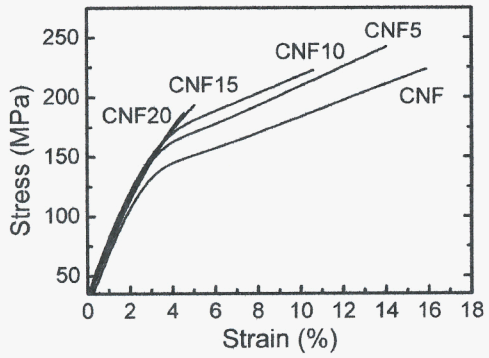

Fig. 4 Typical dry stress–straincurves for CNF and CNF/PF composite films

with high toughness values of 15 MJ/m^3, and they concluded that nanofibrillar networks and high mechanical nanofibril performance control the high toughness. Svagan et al. (2007) reported CNF composites (70 wt % CNF/15 wt % glycerol/15 wt % amylopectin) exhibited high toughness of 9.4 MJ/m^3. The unique high toughness of the composites presented here likely result from a combination of the raw materials, processing and high density. Here, the CNF used to prepare films were obtained from TEMPO-oxidized hardwood fibers under neutral pH conditions. Such fibers have been shown to have uniform nanofibril diameters, high degrees of polymerization (DP) and crystallinity, which contribute to good mechanical properties of resulting films (Saito et al. 2009 ; Johnson et al. 2009). Also, the excess water was removed slowly and gently from the nanofibril suspensions, potentially minimizing residual stresses and defects of the films. Furthermore, the final films were hot-pressed into a dense form. A combination of the raw materials and processing method contributed to the excellent mechanical performance and high toughness of the films reported here.

The wet tensile strength is an important characteristic for cellulosic materials, especially in package and carrier applications (Saito and Isogai 2007). The hydrogen bonds formed between internal cellulose fibers are easily broken down by the permeation of water molecules, which results in a dramatic decrease of tensile strength for CNF films, We tested and compared the wet tensile strength of neat CNF and CNF15 composite films, which were soaked in deionized water for 2.5, 5, 10, and 20 min. The corresponding moisture contents were 78.5, 83.5, 87.1 and 88.6 % for CNF films, and 17.4, 24.2, 27.0 and 29.6 % for CNF15 composite films. Figures 5 and 6, respectively, illustrate the maximum load and elongation at break as functions of soaking times. Since the

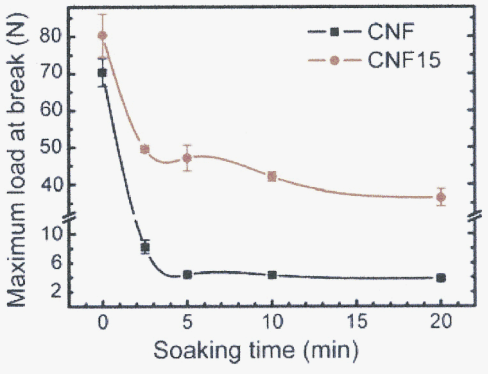

Fig. 5 Maximum load at break for the CNF and CNF15 films as functions of soaking time at wet tensile strength test

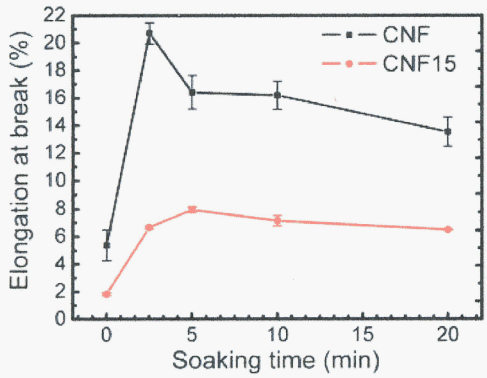

Fig. 6 Elongation at break for the CNF and CMF15 films as functions of soaking time at wet tensile strength test

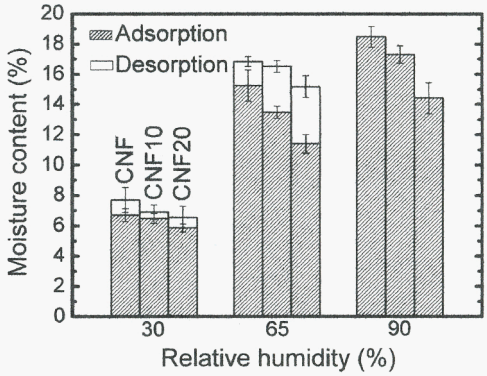

Fig. 7 Absorption (filled column) and desorption (open column) for CNF, CNF10 and CNF20 films

thickness of swelled samples, particularly the neat CNF films, is difficult to measure via conventional methods, here the stresses were not calculated.

A general decrease of maximum load for both neat CNF and CNF15 films is shown in Fig. 5. However, the maximum load at break for CNF15 films varied from 35 to 50 N, which is 7–8 times higher than the neat films. This result indicates addition of PF resin provided some water resistant linkages, such as ether bonds, which reacted between hydroxyl groups in CNFs and methylol groups from PF resin (Nakagaito and Yano 2008), and contributed to the improved wet strength compared to neat CNF films. Furthermore, the cured resin reduced more water permeation into films, resulting in better wet strength.

Interestingly, the elongations for both the neat and composite films soaked in water were increased by more than 300 % compared to the dry ones. This result was comparable with that reported by Sehaqui et al. (2012) in which wet TEMPO-oxidized cellulose nanofibril strips were stretched to as high as 60 %. The weakening of inter-nanofibril bonds facilitates easier and longer draw without breakage (Sehaqui et al. 2012). Water molecules surrounded by nanofibrils also acted as a plasticizer that reduced the stiffness of individual fibers, which facilitated movement between entangled nanofibrils under constant tension (Aulin et al. 2010). Such results indicate that even previously dried CNF sheets may be subject to high fiber orientation and this deserves further investigation.

Moisture and water absorption characteristic

The moisture absorption–desorption characteristic of CNF, CNF10 and CNF20 films is shown in Fig. 7. The moisture contents (MC) for these films were approximately 6–8 %, 13–16% and 14–18% at 30, 65 and 90 % RH, respectively. The increase in MC from 30 to 65 % RH was more dramatic than the increase from 65 to 90 % RH, which is related to the fiber saturation point. Moisture was not readily desorbed when the RH was decreased to 65 %, but the MC returned close to original values when the RH was reduced back to 30 %. As expected, the MC during desorption was higher than during absorption because more hydroxyl groups were made accessible at high MC (Henriksson and Berglund 2007).

CNF films are potentially promising as barrier materials in food package and coating (Syverud and Stenius 2009; Minelli et al. 2010). However, at high humidity hydrogen bonds among adjacent nanofibrils were partially substituted for nanofibril-water hydrogen bonds (Aulin et al. 2010). High MC of CNF films has been shown to increase the oxygen permeability by replacement of nanofibril-water hydrogen bonds (Syverud and Stenius 2009; Aulin et al. 2010). The MC of composites was reduced compared to neat CNF films, especially at higher RH, thus making CNF/PF films potential candidates for barrier films even at high RH.

CNF and CNF/PF films were soaked in deionized water to evaluate the effect of PF resin on water absorption, and the results are shown in Fig. 8. CNF films absorbed approximately 12 times their dry weight in water after 4 h of soaking, and the resulting thickness was about 20 times that of the dry films. The water uptake of the composite films was significantly less than for neat films, and sample CNF15 had relative MC of about 0.5 after soaking for 4 h. Notably, the water absorption primarily occurred during the

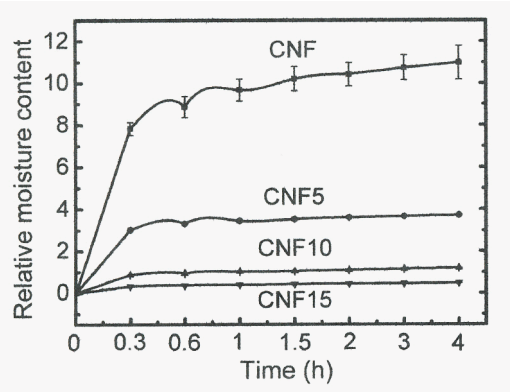

Fig. 8 Evolution of relative moisture contents for CNF and CNF/PF films

first 20 min. Also, water appeared to form small drops on the surface of CNF15 and CNF20 films, indicating dramatically reduced surface energy in the presence of high concentrations of PF resin. These results indicate that the addition of PF resin dramatically decreased the water absorption of CNF films.

In high humidity, hydrogen bonds between nanofibrils of CNF films were easily dissociated by adequate substitution of water-nanofibril bonds, while considerable water molecules were absorbed on the hydroxyl groups and swelled the dense structure. As for CNFPF films, water-resistant PF acted as a barrier to prevent permeation of water. Adhesion between nanofibrils and phenolic OH groups reduced accessibility of hydrophobic groups and their crosslinked chemical bonds limited the extra thickness swelling as well (Nakagaito and Yano 2008 ; Qing et al. 2012).

Oxygen permeability

A summary of the oxygen transmission rates is shown in Table 2 . At 35 % RH, the oxygen transmission rate for the CNFPF composite was dramatically reduced compared to neat CNF films, However, at 100 % RH, the oxygen transmission rate was higher for CNFPF composite films than for neat CNF films. The oxygen transmission rate was roughly four or five orders of magnitude higher at 100 % RH than at 35 % RH. This was not surprising for the neat CNF films as similar results have been previously observed (Minelli et al. 2010 ; Syverud and Stenius 2009 ; Aulin et al. 2010). However, because of the reduced water absorption of CNF/PF composite films, inferior oxygen barrier performance of the composite at high humidity was not expected.

The increased oxygen transmission of the composite as compared to the neat films is also contradictory to the wet tensile data reported above. One possible explanation of the poor oxygen barrier performance on the composite could be oxidative reaction of the PF resin when subjected to continuous, long-term oxygen streams, although such oxidative degradation is typically observed at much higher temperatures (Conley and Bieron 1963). A more likely explanation, however, is that the swelling of CNF resulted in separation of the bonds at the CNF/PF interface, resulting in pathways for oxygen to permeate the films. The PF resin is thought to have penetrated between thin layers of water-swollen CNF, creating layered structures of resin and CNF. The presence of moisture may also disrupt much of the non-chemical bonding between resin and cellulose molecules. Whether similar oxygen transmission results would be found for CNF/PF composites created using other methods, such as described by Qing et al. (2012), is unclear. Further study of the mechanisms resulting in the increased oxygen permeation of the composites in this study is warranted.

Table 2 Oxygen transmission rates

Sample ID	Oxygen transmission rate (cc/m²/24 h)	
	35 % RH	100 % RH
CNF	1.65×10^{-3} (1.0×10^{-4})	13.5 (3.6)
CNF10	2.23×10^{-4} (2.0×10^{-4})	19.5 (1.4)

Values in parenthesis represent standard deviation

Conclusions

Highly flexible CNFPF films were successfully prepared by impregnating water-swollen CNF films with PF resin under ambient conditions. PF uniformly impregnated and adhered to CNFs to improve the mechanical, wet strength, and hygroscopic characteristics. Experimental results showed the highest mechanical properties presented in CNFPF films with addition of 8 wt % PF, and the corresponding tensile strength and toughness were 248 Mpa and 26 MJ/m³ respectively. Moisture absorption of CNF films was reduced, especially at high humidity, and water absorption was dramatically decreased. The wet strength of the CNF films was improved with the

addition of PF resin. The addition of PF resin also decreased the oxygen permeation at 35 % RH. However, despite the composites reduced capacity to absorb water, the oxygen permeation at 100 % RH was not improved. CNF/PF films with high toughness and limited moisture absorption have potential applications as packaging material, or electronic substrates, although further evaluation for these applications is needed.

Acknowledgments Enormous gratitude is offered to Rick Reiner for preparing and supplying TEMPO-oxidized cellulose nanofibrils. The authors would like to acknowledge Benjamin Treml for help with tensile testing. Tom Kuster and Jane O'Dell are kindly acknowledged for SEM and DMTA tests, respectively. The authors would also like to thank Joseph Jakes and Jane O'Dell for performing AFM scans. This work was partly supported by the national "948" project of China (2009-4-51).

References

Andresen M, Johansson L-S, Tanem BS, Stenius P (2006) Properties and characterization of hydrophobized microfibrillated cellulose. Cellulose 13(6):665-677

ASTM (2010a) Annual Book of ASTM Standards, ASTM D638–10: standard test method for tensile properties of plastics. ASTM International, West Conshohockon

ASTM (2010b) Annual Book of ASTM Standards, ASTM D3985-05el: standard test method for oxygen gas transmission rate through plastic film and sheeting using a coulometric sensor. ASTM International, West Conshohockon

Aulin C, Ahola S, Joseffson P, Nishino T, Hirose Y, Österberg M, Wågberg L (2009) Nanoscale cellulose films with different crystallinities and mesostructures-their surface properties and interaction with water. Langmuir 25(13):7675-7685

Aulin C, Gällstedt M, Lindström T (2010) Oxygen and oil barrier properties of microfibrillated cellulose films and coatings. Cellulose 17(3):559–574

Conley RT, Bieron JF (1963) A study of the oxidative degradation of phenol-formaldehyde polycondensates using infrared spectroscopy. J Appl Polym Sci 7(1):103–117

Czaja WK, Young DJ, Kawecki M, Brown RM (2007) The future prospects of microbial cellulose in biomedical applications. Biomacromolecules 8(1):1–12

Fukuzumi H, Saito T, Iwata T, Kumamoto Y, Isogai A (2009) Transparent and high gas barrier films of cellulose nanofibers prepared by TEMPO-mediated oxidation. Biomacromolecules 10(1):162–165

Gong G, Pyo J, Mathew AP, Oksman K (2011) Tensile behavior, morphology and viscoelastic analysis of cellulose nanofiber-reinforced (CNF) polyvinyl acetate (PVAc). Compos Part A 42(9):1275–1282

Henriksson M, Berglund LA (2007) Structure and properties of cellulose nanocomposite films containing melamine formaldehyde. J Appl Polym Sci 106(4):2814–2817

Henriksson M, Berglund LA, Isaksson P, Lindström T, Nishino T (2008) Cellulose nanopaper structure of high toughness. Biomacromolecules 9(6):1579–1585

Iwamoto S, Kai W, Isogai A, Iwata T (2009) Elastic modulus of single cellulose microfibrils from tunicate measured by atomic force microscopy, Biomacromolecules 10(9):2571-2576

Iwatake A, Nogi M, Yano H (2008) Cellulose nanofiber-reinforced polylacitic acid. Compos Sci Technol 68(9):2103–2106

Johnson RK, Zink-Sharp A, Renneckar SH, Glasser WG (2009) A new bio-based nanocomposite: fibrillated TEMPO-oxidized celluloses in hydroxypropylcellulose matrix. Cellulose 16(2):227–238

Lu J, Askeland P, Drzal LT (2008) Surface modification of microfibrillated cellulose for epoxy composite applications. Polymer 49(5):1285–1296

Minelli M, Baschetti MG, Doghieri F, Ankerfors M, Lindström T, Siró I, Plackett D (2010) Investigation of mass transport properties of microfibrillated cellulose (MFC) films. J Membr Sci 358(1–2):67–75

Nakagaito AN, Yano H (2005) Novel high-strength biocomposites based on micro fibrillated cellulose having nano-order-unit web-like network structure. Appl Phys A 80(1):155–159

Nakagaito AN, Yano H (2008) The effect of fiber content on the mechanical and thermal expansion properties of biocomposites based on microfibrillated cellulose. Cellulose 15(4):555–559

Nogi M, Iwamoto S, Nakagaito AN, Yano H (2009) Optically transparent nanofiber paper. Adv Mater 21(16):1595–1598

Nyström G, Mihranyan A, Razaq A, Lindström T, Nyholm L, Strømme M (2010) A nanocellulose polypyrrole composite based on microfibrillated cellulose from wood. J Phys Chem B 114(12):4178-4182

Okahisa Y, Yoshida A, Miyaguchi S, Yano H (2009) Optically transparent wood-cellulose nanocomposite as a base substrate for flexible organic light-emitting diode displays. Compos Sci Technol 69(11–12):1958-1961

Olsson RT, Azizi Samir MAS, Salazar-Alvarez G, Belova L, Ström V, Berglund LA, Ikkala **O**, Nogués J, Gedde UW (2010) Making flexible magnetic aerogels and stiff magnetic nanopaper using cellulose nanofibrils as templates. Nat Nanotechnol 5(8):584–588

Pääkkö M, Vapaavuori J, Silvennoinen R, Kosonen H, Ankerfors M, Lindström T, Berglund LA, Ikkala **O** (2008) Lang and entangled native cellulose I nanofibers allow flexible aerogels and hierarchically porous templates for functionalities. Soft Matter 4(12):2492-2499

Pizzi A, Eaton NJ (1987) A conformational analysis approach to phenol-formaldehyde resins adhesion to wood cellulose. J Adhes Sci Technol 1(1):191–200

Procter HR (1914) The equilibrium of dilute hydrochloric acid and gelatin. J Chem Soc 105:313–327

Qing Y, Sabo R, Wu Y, Cai Z (2012) High-performance cellulose nanofibril composite films. Bio Res 7(3):3064–3075

Rodionova G, Saito T, Lenes M, Eriksen G, Fukuzumi H, Isogai A (2012) Mechanical and oxygen barrier properties of films prepared from fibrillated dispersions of TEMPO-oxidized Norway spruce and Eucalyptus pulps. Cellulose 19(3):705–711

Sabo R, Seo JH, Ma Z (2012) Cellulose nanofiber composite substrates for flexible electronics, 2012 TAPPI International Conference on Nanotechnology for Renewable Materials. Montreal, Quebec

Saito T, Isogai A (2007) Wet strength improvement of TEMPO-oxidized cellulose sheets prepared with cationic polymers. Ind Eng Chem Res 46(3):773–780

Saito T, Hirota M, Tamura N, Kimura S, Fukuzumi H, Heux L, Isogai A (2009) Individualization of nano-sized plant cellulose fibrils by direct surface carboxylation using TEMPO catalyst under neutral conditions. Biomacromecules 10(7):1992–1996

Sasso C, Zeno E, Petit-Coni1 M, Chaussy D, Belgacem MN, Tapin-Lingua S, Beneventi D (2010) Highly conducting polypyrrole/cellulose nanocomposite films with enhanced mechanical properties. Macromol Mater Eng 295(10): 934–941

Sehaqui H, Mushi NE, Morimune S, Salajkova M, Nishino T, Berglund LA (2012) Cellulose nanofiber orientation in nanopaper and nanocomposites by cold drawing. ACS Appl Mater Interfaces 4(2): 1043–1049

Shimazaki Y, Miyazaki Y, Takezawa Y, Nogi M, Abe K, Ifuku S, Yano H (2007) Excellent thermal conductivity of transparent cellulose nanofiber/epoxy resin nanocomposites. Biomacromolecules 8(9):2979-2978

Siró I, Plackett D (2010) Microfibrillated cellulose and new nanocomposites materials: a review. Cellulose 17(3):459–494

Svagan AJ, Azizi Samir MAS, Berglund LA (2007) Biomimetic polysaccharide nanocomposites of high cellulose content and high toughness. Biomacromolecules 8(8):2556–2563

Syverud K, Stenius P (2009) Strength and barrier properties of MFC films. Cellulose 16(1):75-85

Tingaut P, Zimmermann T, Lopez-Suevos F (2010) Synthesis and characterization of bionancomposites with tunable properties from poly (lactic acid) and acetylated microfibrillated cellulose. Biomacromolecules 11(2):454–464

Zhu J, Sabo R, Luo X (2011) Integrated production of nanofibrillated cellulose and biofuel (ethanol) by enzymatic fractionation of wood fibers. Green Chem 13(5):1339–1344